Hindawi
Shock and Vibration
Volume 2021, Article ID 6971178, 10 pages
https://doi.org/10.1155/2021/6971178

Research Article

A New Radial Spoiler for Suppressing Vortex-Induced Vibration of a Tubular Tower and Its Practical Design Method

Xing Fu,[1,2] **Yao Jiang**,[1] **Wen-Long Du**,[1] **and Bo-Wen Yan**[2,3]

[1]*State Key Laboratory of Coastal and Offshore Engineering, Dalian University of Technology, Dalian 116023, China*
[2]*Key Laboratory of New Technology for Construction of Cities in Mountain Area, Ministry of Education, Chongqing University, Chongqing 400045, China*
[3]*Chongqing Key Laboratory of Wind Engineering and Wind Energy Utilization, School of Civil Engineering, Chongqing University, Chongqing 400045, China*

Correspondence should be addressed to Bo-Wen Yan; bowenyancq@cqu.edu.cn

Received 28 July 2021; Accepted 31 August 2021; Published 27 September 2021

Academic Editor: Bing Qu

Circular section tubular members with smaller wind load shape coefficient and higher stability are widely used in ultra-high-voltage (UHV) transmission towers. However, the tubular members, especially those with a large slenderness ratio, are prone to vortex-induced vibration (VIV) within a specific wind speed range. The sustained vibration of members can easily cause fatigue failure of joints and threaten the operational safety of transmission lines. Consequently, a novel countermeasure for the VIV of tubular towers using a new type of radial spoiler is proposed, whose mechanism is to change the vortex shedding frequency by destroying the large-scale vortexes into small-scale vortexes. Then, the parametric analysis of different variables is carried out based on the orthogonal experiment and numerical simulation, including the height H and length B of the spoiler and the distance S between adjacent spoilers. The results show that the above three parameters all have significant influences on vortex shedding frequency. Additionally, a practical design method of the new radial spoiler is proposed, and the recommended values of H, B, and S are $1D$~$2D$, $1.5H$~$3H$, and $5D$~$12.5D$, respectively, where D is the diameter of the tubular member. Finally, a numerical verification of the suppression effects is carried out, demonstrating that the proposed quick design method is simple and reliable, which can be widely used in the VIV design of tubular towers.

1. Introduction

The ultra-high-voltage (UHV) transmission project has the advantages of long transmission distance, large transmission capacity, and low power loss [1, 2], which dramatically drives technological innovation. Tubular members can increase the bearing capacity and reduce the weight of tower. Therefore, tubular towers are widely used in UHV transmission lines [3, 4].

Nevertheless, the wind will produce shedding vortexes on the leeward side of tubular members alternately within a specific wind speed range [5]. When the shedding frequency of the vortexes is close to the natural frequency of tubular members, the vortex-induced vibration (VIV) occurs, usually accompanied by larger amplitude vibrations. Long-term repetitive vibration may cause the looseness of bolts and the fatigue failure of welds [6], which will affect the operational safety of transmission lines. Consequently, for tubular towers, the prevention and control of the VIV are essential.

The control methods of the VIV are mainly divided into two categories: active control and passive control. The former applies the external forces on the structure automatically through a real-time monitoring system, while the latter adjusts the vortex shedding frequency [7] by altering the aerodynamic shape of the structure. The purpose of both is to interfere with the flow field. Passive control is widely used in practice due to its simple principle and treatment compared with active control. Zdravkovich [8] divided the passive controls into three categories: (1) surface protrusions (helical strakes, fins, etc.); (2) shrouds (perforated shells,

axial rods, etc.); (3) near-wake stabilizers (guiding plates, vanes, etc.), which open the minds for future research. Stansby et al. [9] introduced a spoiler design suitable for the marine environment, whose effectiveness was verified through a model test. Chen et al. [10] found that, for a flexible riser, a positive VIV suppression effect can be achieved by installing the helical strakes with a reasonable geometrical configuration. Larsen et al. [11] found that the VIV of bridges can be significantly suppressed by the guide plate, and guide vane arrangements are proved to be equally efficient for other shallow box girders with the correct installation method.

Currently, VIV countermeasures are mainly concentrated on ocean and bridge engineering, ignoring electric power engineering, especially the tubular transmission towers. For tubular towers, stiffening cables are usually used to suppress the VIV via reducing the deformation and the slenderness ratio of tubular members; two ends are fixed on the main members and the tubular members, respectively. However, this method has not yet been employed widely due to the need for connection plates reserved on the main members. Consequently, Jingbo et al. [12] proposed a parameter design method of the antivibration hammer to suppress the VIV of tubular members, which has a positive effect. However, its application is restricted due to the lack of a mature algorithm for the damping of steel strand current.

Based on previous studies, a new type of radial spoiler is proposed to suppress the VIV of tubular towers. Then, the parameters of the spoiler are analyzed, and a design method is given based on numerical simulation and orthogonal experiment. Finally, two cases are taken to verify the applicability of the design method.

2. A New Radial Spoiler for the VIV Control

2.1. Detailed Description. In this section, a new type of radial spoiler (after this referred to as "spoiler" for convenience) based on the passive control method is proposed. A spoiler comprises two half steel pipes (the steel type is Q345, with the elastic modulus of 206 GPa and the yield strength of 345 MPa) connected by high-strength bolts. Three same steel plates, with a width of H, a length of B, and a thickness of 3 mm, are welded on each half steel pipe at equal intervals. The distance between the adjacent spoilers is S. Rubber gaskets are arranged between the tubular members and spoilers to increase the contact area and avoid loosening. The specific design is shown in Figure 1.

2.2. Case Verification and Suppression Mechanism. To reveal the suppression mechanism of the proposed method, the VIV of a tubular member is simulated. A member with a large slenderness ratio is selected, with an outer diameter D of 159 mm, an inner diameter d of 151 mm, a length L of 8320 mm, and a mass $\overline{m}$ of 15.26 kg/m, which is more prone to the VIV. The connection style of the joint is shown in Figure 2, and the x-axis and y-axis are the strong transverse direction and weak transverse direction, respectively.

Some related research illustrates that the response of strong transverse direction can be ignored when the VIV occurs in the members whose joints are connected by the style shown in Figure 2 [13]. Accordingly, only the response of weak transverse direction is considered. The vibration in the weak transverse direction can be simplified as a continuous beam hinged at both ends; hence, the natural circle frequency $\omega_n = \pi^2/L^2\sqrt{EI/\overline{m}}$; i.e., the natural frequency $f_n = \omega_n/2\pi$. The wind speed U corresponding to the VIV can be obtained from

$$U = \frac{f_s D}{St}, \tag{1}$$

where f_s is vortex shedding frequency and St is the Strouhal number, equaling 0.21 in the subcritical region [14]. When the VIV occurs, $f_s = f_n$, $U = 6.3 \times 0.159/0.2 \approx 5$ m/s.

To accurately simulate the vortex-induced force of wind field acting on the tubular member, the calculation domain and the mesh are set up accurately, as shown in Figure 3. The calculation domain is set as 28 $D \times 16$ $D \times L$; the distance between the tubular member and inlet, outlet, upper, and lower is 8D, 20D, 8D, and 8D, respectively, while the influence of blocking rate can be ignored [15]. The boundary conditions are velocity inlet and pressure outlet; the upper, lower, left, and right boundary conditions are symmetrical. The surface boundary condition of the tubular member is slip wall.

Previous researches had shown that the spanwise grid height needs to be less than 0.0065D to capture more accurate simulation results for the flow around a three-dimensional cylinder [16]. Thus, the spanwise grid height is set as 0.006D in this paper. The selected turbulence model is large-eddy simulation (LES) technique, which is more precise than the Reynolds-average Navier-Stokes (RANS) technique in three-dimensional simulation [17]. PISO algorithm is used to solve the coupling problem of pressure and velocity, and the least-squares cell-based method is applied for gradient interpolation. The second-order implicit scheme is employed for transient scheme, and the second-order scheme is used for pressure difference and momentum difference. The height of the first mesh layer is set as 3.79×10^{-5} m to satisfy the condition that the nondimensional wall distance y^+ is less than 1 [18], and the iteration time step is 2×10^{-4} s.

Figure 4 displays the time history of the lift coefficient C_l, where C_l is defined as $C_l = F_l/0.5\rho_a U^2 D$, F_l is lift force, and ρ_a is air density. It can be noticed that the lift coefficient oscillates periodically and the amplitude has obvious three-dimensional pulsation characteristics, which is due to the influence of spanwise spatial characteristics of flow field. The vortex shedding frequency f_s can be obtained from the power spectral density (PSD) curve of the lift coefficient, as shown in Figure 5. At that point, $f_s = f_n = 6.3$ Hz, which is close to the member's natural frequency, and the structural resonance occurs under the action of VIV.

Table 1 compares the simulation results and the results obtained from Norberg's wind tunnel test [19].

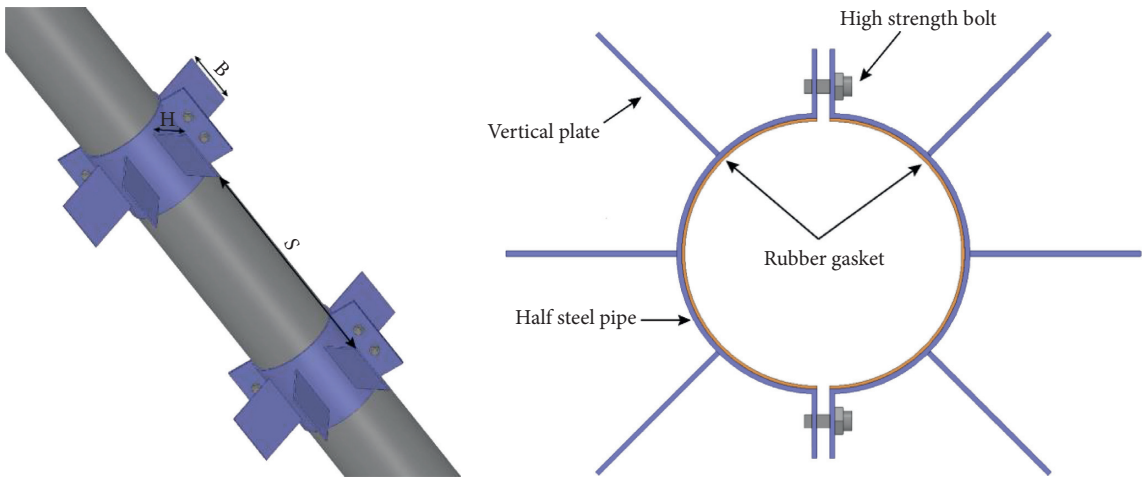

Figure 1: The design scheme of the new spoiler. (a) Basic parameters. (b) Geometric details of the spoilers.

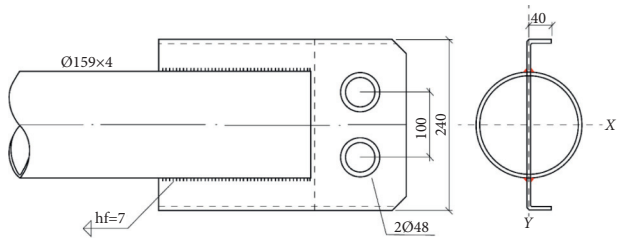

Figure 2: The connection style of the joint.

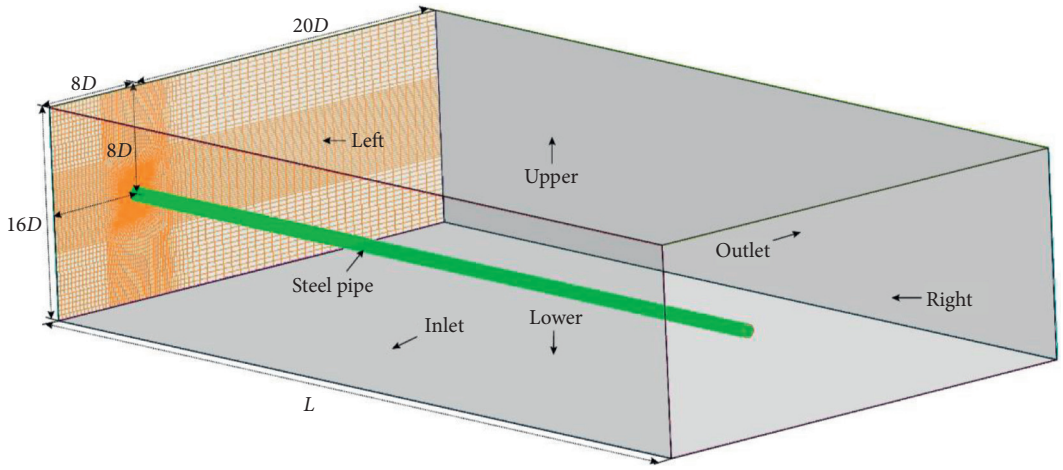

Figure 3: The computational domain and mesh generation.

The Reynolds number of this experiment was about 25000. Compared with the data of Norberg's wind tunnel under this Reynolds number, it is found that the average drag coefficient $\overline{C}_d$, Strouhal number St, and the root mean square of the lift coefficient RMS_{Cl} are very close, which indicates the reliability of numerical simulation results. Consequently, grid independence verification will not be carried out in the following research.

To reveal the suppression mechanism of the spoiler, two spoilers are installed on the member for numerical simulation. The parameters are as follows: $H = 100$ mm, $B = 300$ mm, and $S = 800$ mm. The calculation model is shown in Figure 6. The corresponding time history and PSD of the lift coefficient are shown in Figures 7 and 8, respectively. It can be seen that the lift coefficient amplitude decreases obviously with the spoilers installed, and f_s

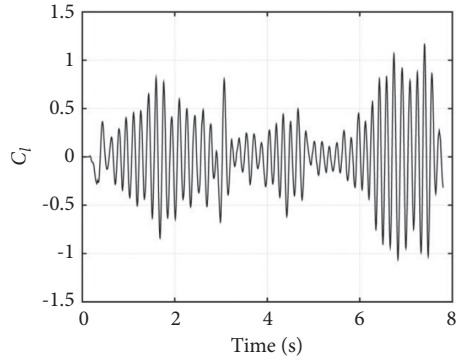

Figure 4: Time history of lift coefficient.

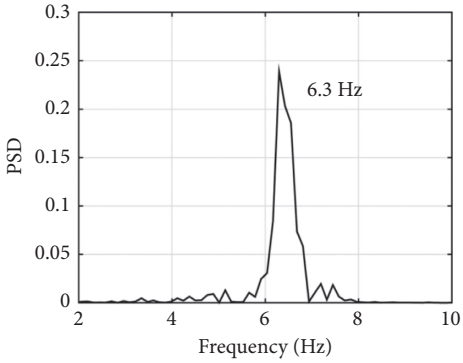

Figure 5: PSD of lift coefficient.

Table 1: Comparison of experimental and numerical results.

Method	$\overline{C}_d$	St	RMS_{Cl}
Numerical simulation	1.17	0.19	0.47
Norberg's test	1.19	0.19	0.49
Relative error	1.7%	0.0%	4.1%

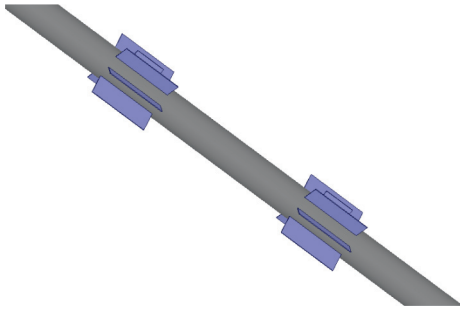

Figure 6: The calculation model with two spoilers.

decreases from 6.3 Hz to 1.15 Hz, which avoids resonance by making the vortex shedding frequency away from the member's natural frequency. The VIV is suppressed, indicating the availability of the spoilers.

Figure 9 reveals the contour of vortex cores with the spoilers. The spoilers destroy the large-scale vortexes into small-scale vortexes, which weaken the intensity of vortexes

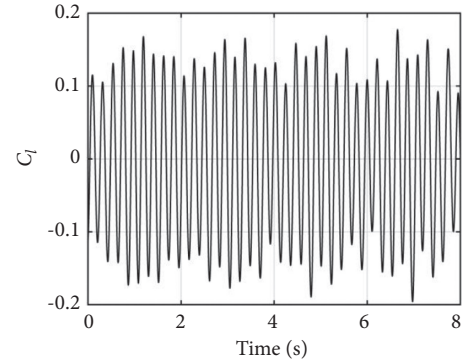

Figure 7: Time history of lift coefficient (with spoilers).

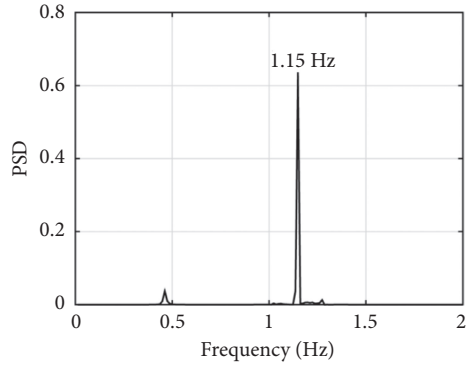

Figure 8: PSD of lift coefficient (with spoilers).

and reduce the fluid forces, and this is the primary suppression mechanism of the spoiler toward the VIV.

3. Parametric Analysis

In Technical Regulations of the Design of Steel Tubular Towers of Overhead Transmission Lines (DL/T5254-2010) [20], the VIV can be limited by reducing the slenderness ratio to increase the first-order vibration critical wind speed of tubular members, but this method will increase the weight of the tower prominently. Therefore, some members are still selected with a large slenderness ratio in the practical design. Thus, VIV still occurs under certain conditions. Based on a wind tunnel test, Jing-Bo et al. [21] pointed out that the VIV can be restrained by installing some axially distributed short ribs on the surface of steel tubes, or replacing circular cross section steel tubes with multi-ribbed steel tubes. However, only conceptual design cannot meet practical engineering needs.

The spoiler for VIV suppression proposed in this paper has a good effect with the advantages of easy installation, simple processing, and convenient transportation. The parametric analysis of H, B, and S of the spoiler is carried out next to provide a design method for the prevention of the VIV of tubular towers.

3.1. Orthogonal Experiment. Orthogonal experimental design is a method to study multiple factors and multiple levels by selecting some representative points from the

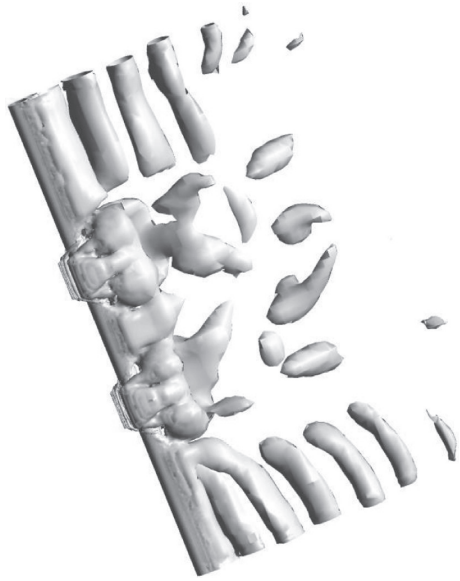

Figure 9: Vortex cores (with spoilers).

comprehensive test according to the orthogonality. Orthogonal experimental design can significantly reduce the number of tests; that is because the selected representative points have the characteristics of uniform dispersion. Therefore, this method has been widely used in a multitude of fields.

To explore the influence of H, B, and S on the vortex shedding frequency, five different levels (No. 1–5) are set for each factor. 125 (5^3) groups of numerical experiments need to be carried out if the conventional method of control variates is adopted, which will consume an abundance of computing resources and time on account of the complexity and high consumption of resources of the 3D simulation wind field. Therefore, the orthogonal experimental design and some representative experiments are employed to optimize the simulation scheme.

Set $H = a\ D$, $B = bH$, and $S = c\ D$ with the intention of facilitating the research and expression. Consequently, Table 2 displays the factors a, b, and c with five levels. We optimize the experiment scheme via applying a $L_{25}(5^2)$ orthogonal experiment table, and the simulation number is reduced from 125 to 25, of which the simulation scheme is shown in Table 3.

H, B, and S are rounded upward for the convenience of processing in practical engineering. The evaluation index of the suppression effect is measured by the vortex shedding frequency f_s, and FLUENT is employed to perform 25 numerical tests with the same calculation method in Section 1. Case No.12 is designated as an example to demonstrate the simulation process. The levels of the factors a, b, and c are 2, 2, and 3, respectively, and $a = 0.65$, $b = 1.5$, $c = 10$, i.e., $H = a\ D = 100$ mm, $B = bH = 150$ mm, and $S = c\ D = 1600$ mm. In order to reduce the amount of calculation, the height of the calculation domain is set as 6 m, as shown in Figure 10, and two spoilers are installed for parametric analysis.

The lift coefficient C_l is obtained from the simulation results, and the vortex frequency f_s can be obtained from the PSD of C_l. The results of the 25 cases are set out in Figure 11. The value above the blue bar is the vortex frequency f_s of each case, and the red horizontal line indicates the vortex frequency without spoilers; i.e., $f_s = f_n = 6.3$ Hz. It can be seen that there are apparent suppression effects in every case, verifying the effectiveness of the spoilers again. Theoretically, the greater the difference between f_s and f_n, the better the suppression effect. For the convenience of designers, the vortex frequency f_s is linearly converted to the corresponding score SC; i.e., $SC = 100 - 100 f_s / f_n$. The limit f_s is 0 Hz, and $SC = 100$. Figure 11 is converted to Figure 12 with this rule.

Table 2: Factors and levels.

Level	Factors		
	a	b	c
1	0.2	1	5
2	0.65	1.5	7.5
3	1.1	2	10
4	1.55	2.5	12.5
5	2	3	15

3.2. Result Analysis. In order to further analyze the contribution of various factors and levels to the suppression of vortex shedding, the extremum difference analysis method with the advantages of simple calculation and intuitive image is applied to analyze the results of the orthogonal experiments, including calculation and judgment. The calculation includes the extremum difference and experiment indexes. The extremum difference can be calculated by

$$R_j = \max\left(K_{j1}, K_{j2}, K_{jm}\right) - \min\left(K_{j1}, K_{j2}, K_{jm}\right) \quad j = a, b, c\ m = 1, 2, 3, 4, 5, \tag{2}$$

where K_{jm} is the sum of the experiment indexes corresponding to the m level of the factor j, i.e., the sum of SC, and R_j is the extremum difference of the factor j.

The optimal level of the factor j and the optimal level combination of each factor can be judged by the size of K_{jm}. R_j reflects the change range of the experiment index when factor j level changes. The larger the R_j is, the greater the influence of this factor on the index is, and the more paramount it is. Consequently, the primary and secondary factors can be judged according to the size of R_j. The calculation and judgment of the extremum difference analysis are directly carried out in Table 4.

For the sake of more intuitively reflecting the influence law and trend of each factor and level on f_s, the trend chart of level and K_{jm} is drawn with level as abscissa and K_{jm} as ordinate, as shown in Figure 13.

4. Design Method and Numerical Verification

4.1. Practical Design Method. According to the magnitude of extreme difference, the primary and secondary sequence of the three factors is $a > b > c$, i.e., $H > B > S$. The optimal level

Table 3: Simulation scheme.

Case number	Factors		
	a	b	c
1	1	1	1
2	2	5	1
3	3	4	1
4	4	3	1
5	5	2	1
6	1	2	2
7	2	1	2
8	3	5	2
9	4	4	2
10	5	3	2
11	1	3	3
12	2	2	3
13	3	1	3
14	4	5	3
15	5	4	3
16	1	4	4
17	2	3	4
18	3	2	4
19	4	1	4
20	5	5	4
21	1	5	5
22	2	4	5
23	3	3	5
24	4	2	5
25	5	1	5

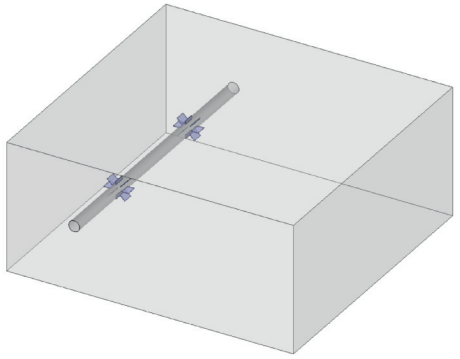

Figure 10: The calculation domain (with spoilers, case No. 12).

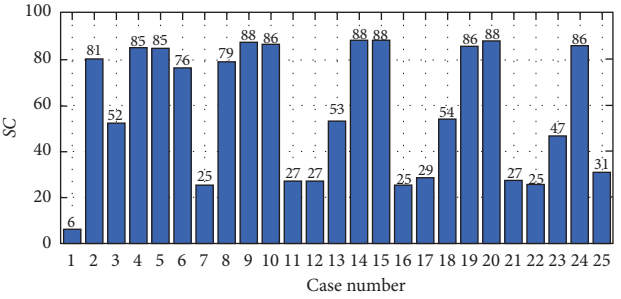

Figure 12: The values of SC with different case number.

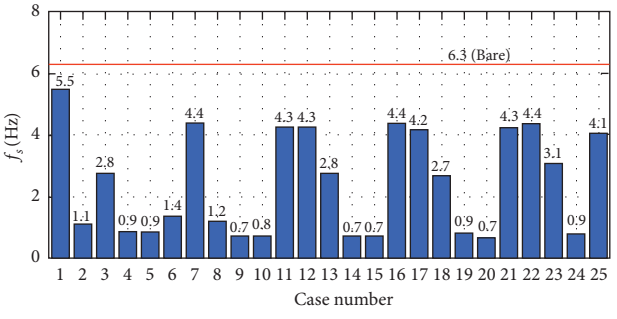

Figure 11: The values of f_s with different case number.

Table 4: Result analysis.

Index	Factors		
	a	b	c
K_{j1}	161	201	309
K_{j2}	187	328	354
K_{j3}	285	274	283
K_{j4}	433	278	280
K_{j5}	378	363	216
R_j	272	162	138
Primary and secondary order	1	2	3
Best level combination	4	5	2

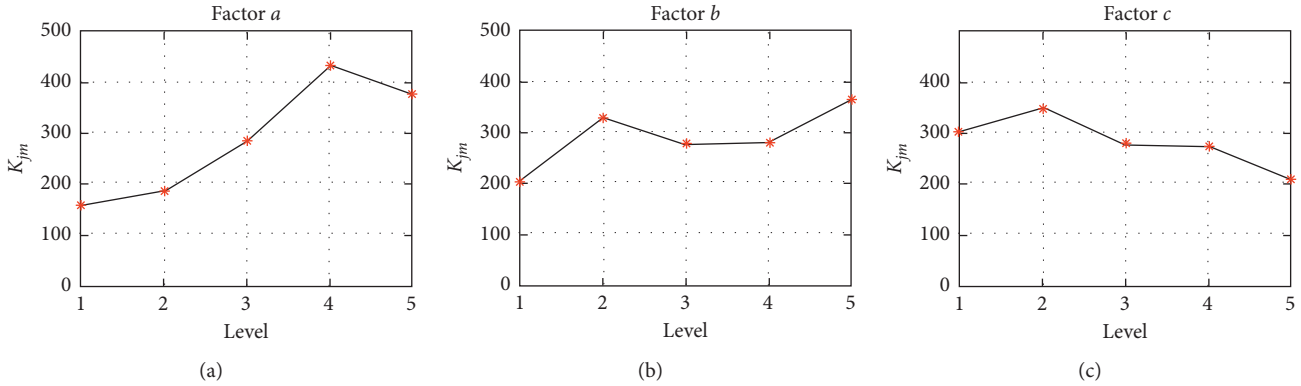

Figure 13: The level and K_{jm} trend diagrams of each factor. (a) Factor a. (b) Factor b. (c) Factor c.

combination is the fourth level of factor a, the fifth level of factor b, and the second level of factor c; i.e., $H = 1.55\ D$, $B = 3H$, $S = 7.5\ D$. Vortex shedding does not need to be completely suppressed for practical engineering design, only to keep the vortex shedding frequency away from the member's natural frequency. Generally, the 50% suppression effect meets the engineering requirements, and the corresponding score SC is greater than or equal to 250 points. Therefore, the design method of the spoiler is as follows according to the trend diagram:

$$H = 1\ D \sim 2\ D, \tag{3}$$

$$B = 1.5H \sim 3H, \tag{4}$$

$$S = 5\ D \sim 12.5\ D. \tag{5}$$

Based on the previous research, the design process of the spoiler is sorted out, as proved in Figure 14. Firstly, the outer diameter D of the tubular member is determined; then the height H and width B of the spoiler are determined according to equations (3) and (4); then the distance S between the adjacent spoilers is determined according to equation (5). Additionally, the number m of the spoilers is determined combined with the length L of the member.

The parameter m should satisfy the following formula: $mB + (m-1)S < L$, i.e., $m < (L+S)/(B+S)$, and it is rounded down to avoid the spoilers being too close to the gusset plate. When m is even, one spoiler is set on both sides at the distance $S/2$ from the center, and then every S is evenly set on both sides. When m is odd, one spoiler is set in the center of the member, and then every S is evenly set on both sides.

4.2. Numerical Verification

4.2.1. Example 1. To validate the applicability of the design method, the tubular members used in Deng's wind tunnel test are selected [22]. The basic parameters are as follows: $D = 70$ mm, $L = 4598$ mm, the slenderness ratio $\lambda = 200$, and the joint style is the same as Figure 2. According to the design method proposed in the previous section, the size of

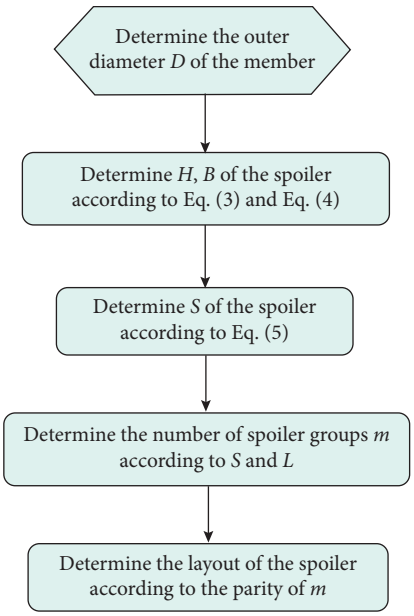

Figure 14: Design process of the proposed spoiler.

the spoilers is selected as $H = 1.5\ D = 105$ mm, rounded up to 110 mm, $B = 2\ H = 220$ mm, $S = 12.5D = 875$ mm, rounded up to 900 mm; the layout scheme is demonstrated in Figure 15.

In Deng's wind tunnel test, the wind speed is 3.5 m/s when the VIV occurs, and the amplitude in the weak transverse direction is the largest. The natural frequency in the weak transverse direction is 10.2 Hz. On employing the method in Section 1, the height of the first mesh layer is 4.82×10^{-5} m, and iteration time step is 2×10^{-4} s. Figure 16 displays the comparison of the lift coefficient and its PSD before and after the installation of spoilers. The vortex shedding frequency is 10.28 Hz without the spoilers, which is close to the member's natural frequency. After the spoilers are installed, the vortex shedding frequency is reduced to 2.27 Hz, which is away from the member's natural frequency.

4.2.2. Example 2. In addition, the auxiliary member with a small slenderness ratio is selected to verify the effectiveness of the method. The basic parameters are as follows:

Figure 15: The layout of Example 1.

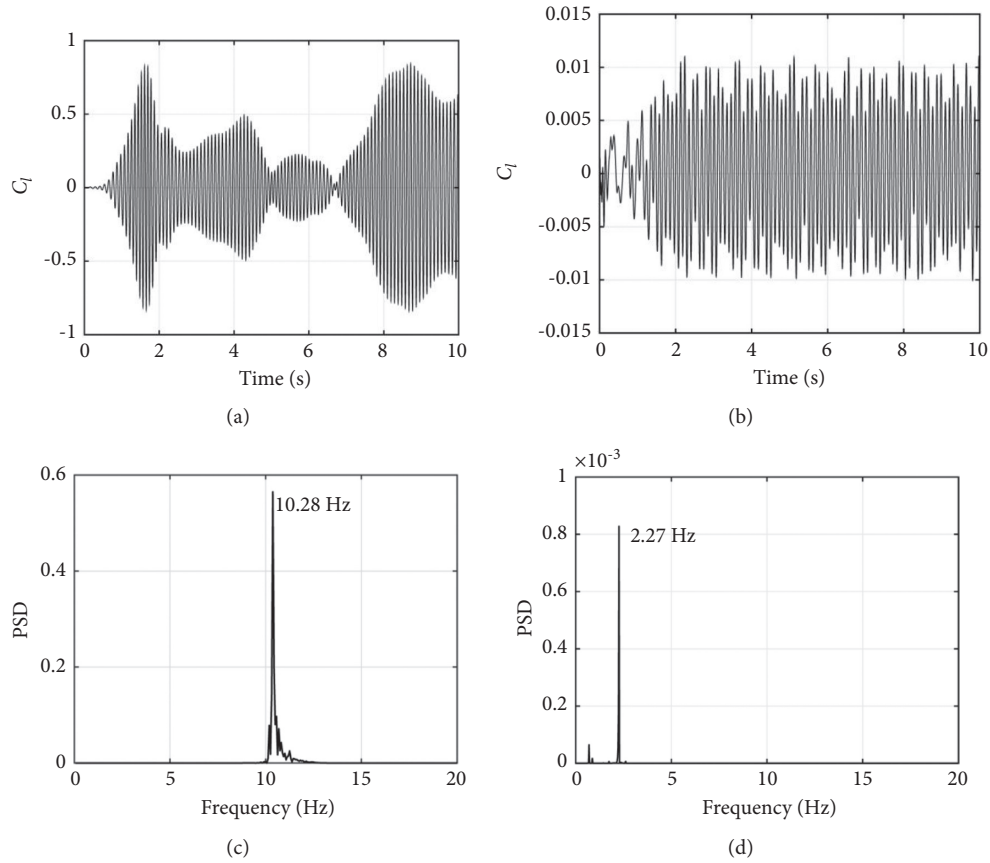

Figure 16: Comparison of lift coefficient and PSD with and without spoilers for Example 1. (a) Time history of lift coefficient (bare). (b) Time history of lift coefficient (with spoilers). (c) PSD of the lift coefficient (bare). (d) PSD of the lift coefficient (with spoilers).

Figure 17: The layout of Example 2.

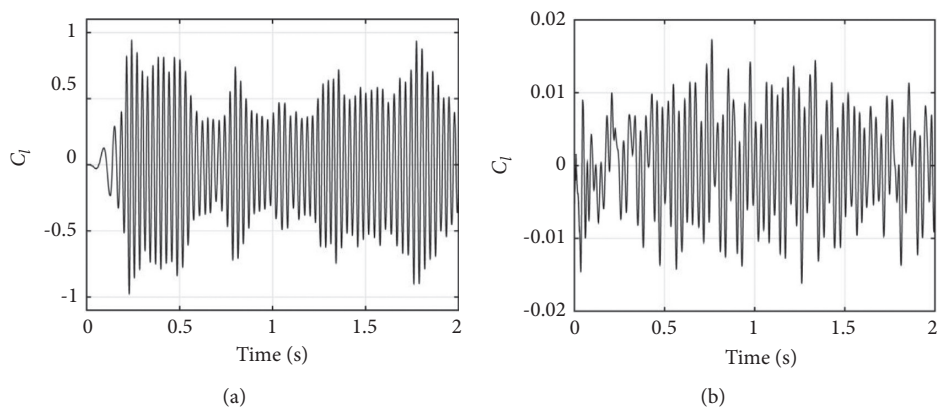

Figure 18: Continued.

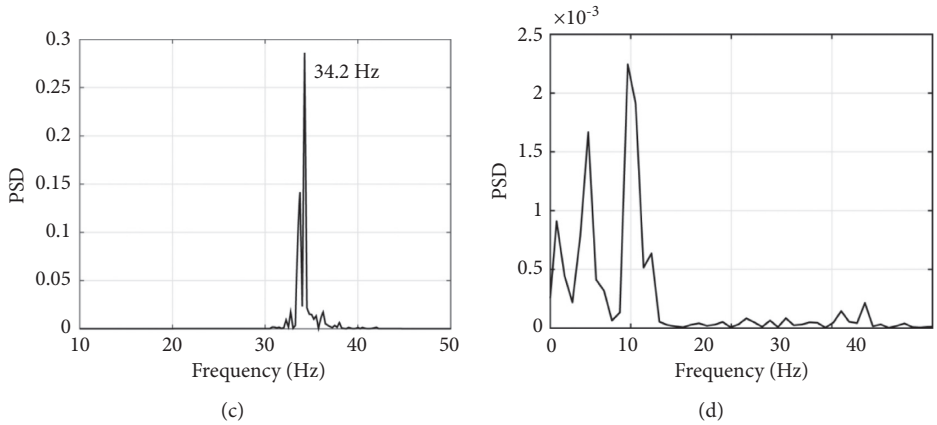

Figure 18: Comparison of lift coefficient and PSD with and without spoilers for Example 2. (a) Time history of lift coefficient (bare). (b) Time history of lift coefficient (with spoilers). (c) PSD of the lift coefficient (bare). (d) PSD of the lift coefficient (with spoilers).

$D = 70$ mm, $L = 2354$ mm, the slenderness ratio $\lambda = 100$, and the joint style is the same as Figure 2. The natural frequency in the weak transverse direction is 34.19 Hz. The spoiler scheme is the same as case 1 due to the same diameter, as shown in Figure 17.

Figure 18 compares the lift coefficient and its PSD with and without the spoilers. The vortex shedding frequency is 34.2 Hz without the spoilers, which is close to the natural frequency of the member, and the VIV occurs, while the dominant frequency of vortex shedding frequency is reduced to 10 Hz installing the spoilers, and the VIV is suppressed.

In the above two cases, the suppression effects of VIV are all obvious, proving the effectiveness of the quick design method, which can be widely used in practical engineering.

5. Concluding Remarks

This study proposed a new type of radial spoiler to suppress the VIV of tubular towers. The suppression mechanism of the spoilers is revealed. Meanwhile, the effectiveness is verified with the aid of numerical simulation method. Then, the practical design method is given based on the parametric analyses of the height H, length B, and distance S conducted by the orthogonal experiment. Finally, the applicability of the design method is verified by two examples. The main conclusions can be summarized as follows:

(1) The new type of spoilers can effectively suppress the VIV of tubular members, and the suppression mechanism is that the spoilers can destroy the vortex structures and reduce the vortex shedding frequency.

(2) The recommended values of H, B, and S are $1D$~$2D$, $1.5H$~$3H$, and $5D$~$12.5D$, respectively. The design scheme of the spoiler can be obtained through the outer diameter D of the member quickly.

(3) The applicability of the design method is verified through two examples, and the results show that the design method is simple and reliable, which provides a new idea for the prevention and control of VIV in tubular towers.

Data Availability

The data of member dimensions and numerical simulations used to support the findings of this study are included within the article.

Conflicts of Interest

The authors declare that they have no conflicts of interest.

Acknowledgments

This research was supported by the Opening Fund of Key Laboratory of New Technology for Construction of Cities in Mountain Area, Ministry of Education (grant no. LNTCCMA-20210112) and the National Natural Science Foundation of China (grant no. 52078104).

References

[1] X. Fu, H.-N. Li, G. Li, Z.-Q. Dong, and M. Zhao, "Failure analysis of a transmission line considering the joint probability distribution of wind speed and rain intensity," *Engineering Structures*, vol. 233, Article ID 111913, 2021.

[2] S. Liang, L. Zou, D. Wang, and H. Cao, "Investigation on wind tunnel tests of a full aeroelastic model of electrical transmission tower-line system," *Engineering Structures*, vol. 85, pp. 63–72, 2015.

[3] L. Tian, J. Liu, C. Chen, L. Guo, M. Wang, and Z. Wang, "Experimental and numerical analysis of a novel tubular joint for transmission tower," *Journal of Constructional Steel Research*, vol. 164, Article ID 105780, 2020.

[4] M. Zhang, G. Zhao, and J. Li, "Nonlinear dynamic analysis of high-voltage Overhead transmission lines," *Shock and Vibration*, vol. 2018, pp. 1–35, 2018.

[5] F. Wang, K. Du, J. Sun, F. Huang, and Z. Xiong, "Shaking table Array tests of an ultra-high-voltage cup-type transmission tower-line system," *Shock and Vibration*, vol. 2019, pp. 1–20, 2019.

[6] X. Fu, H.-N. Li, G. Li, and Z.-Q. Dong, "Fragility analysis of a transmission tower under combined wind and rain loads," *Journal of Wind Engineering and Industrial Aerodynamics*, vol. 199, Article ID 104098, 2020.

[7] G. S. Baarholm, C. Martin Larsen, and H. Lie, "Reduction of VIV using suppression devices—an empirical approach," *Marine Structures*, vol. 18, no. 7, pp. 489–510, 2005.
[8] M. M. Zdravkovich, "Review and classification of various aerodynamic and hydrodynamic means for suppressing vortex shedding," *Journal of Wind Engineering and Industrial Aerodynamics*, vol. 7, no. 2, pp. 145–189, 1981.
[9] P. K. Stansby, J. N. Pinchbeck, and T. Henderson, "Spoilers for the suppression of vortex-induced oscillations (Technical note)," *Applied Ocean Research*, vol. 8, no. 3, pp. 169–173, 1986.
[10] D.-Y. Chen, L. K. Abbas, G.-P. Wang, X.-T. Rui, and W.-J. Lu, "Suppression of vortex-induced vibrations of a flexible riser by adding helical strakes," *Journal of Hydrodynamics*, vol. 31, no. 3, pp. 622–631, 2019.
[11] A. Larsen, S. Esdahl, J. E. Andersen, and T. Vejrum, "Storebælt suspension bridge–vortex shedding excitation and mitigation by guide vanes," *Journal of Wind Engineering and Industrial Aerodynamics*, vol. 88, no. 2, pp. 283–296, 2000.
[12] Y. Jingbo, L. Xilai, D. Songtao et al., "Study on suppression method with dampers against vortex-shedding induced wind vibration of transmission steel tubular tower members," *Building Structure*, vol. 46, no. 14, pp. 30–35, 2016.
[13] H. Deng and Z. Zhao, "Numerical simulation of vortex-induced vibration of steel tubular members in transmission tower," *Journal of Tongji University*, vol. 45, no. 1, pp. 9–15, 2017.
[14] C. H. K. Williamson and R. Govardhan, "A brief review of recent results in vortex-induced vibrations," *Journal of Wind Engineering and Industrial Aerodynamics*, vol. 96, no. 6-7, pp. 713–735, 2008.
[15] X. Fu, H.-N. Li, and T.-H. Yi, "Research on motion of wind-driven rain and rain load acting on transmission tower," *Journal of Wind Engineering and Industrial Aerodynamics*, vol. 139, pp. 27–36, 2015.
[16] P. Parnaudeau, J. Carlier, D. Heitz, and E. Lamballais, "Experimental and numerical studies of the flow over a circular cylinder at Reynolds number 3900," *Physics of Fluids*, vol. 20, no. 8, pp. 212–287, 2008.
[17] J. Franke and W. Frank, "Large eddy simulation of the flow past a circular cylinder at ReD=3900," *Journal of Wind Engineering and Industrial Aerodynamics*, vol. 90, no. 10, pp. 1191–1206, 2002.
[18] X. Fu, W.-L. Du, H.-N. Li, G. Li, Z.-Q. Dong, and L.-D. Yang, "Stress state and failure path of a tension tower in a transmission line under multiple loading conditions," *Thin-Walled Structures*, vol. 157, Article ID 107012, 2020.
[19] C. Norberg, "Flow around a circular cylinder: aspects of fluctuating lift," *Journal of Fluids and Structures*, vol. 15, no. 3, pp. 459–469, 2001.
[20] *Technical Regulations of the Design of Steel Tubular Towers of Overhead Transmission lines National Energy Administration*, Beijing, China, 2011.
[21] Y. Jing-Bo, L. Zheng, and W. Jing-Chao, "Prevention of steel tube UHV transmission tower aeolian vibration," *Electric Power Construction*, vol. 29, no. 9, pp. 10–13, 2008.
[22] H. Z. Deng, Q. Jiang, F. Li, and Y. Wu, "Vortex-induced vibration tests of circular cylinders connected with typical joints in transmission towers," *Journal of Wind Engineering and Industrial Aerodynamics*, vol. 99, no. 10, pp. 1069–1078, 2011.